

# Experimental measurements of a prototype vibraphone bar with three-dimensional cutaway geometry <sup>EP</sup>

Cite as: JASA Express Lett. 2, 083201 (2022); <https://doi.org/10.1121/10.0013470>

Submitted: 22 June 2022 • Accepted: 26 July 2022 • Published Online: 12 August 2022

 Douglas Beaton and Gary Scavone

## COLLECTIONS

 This paper was selected as an Editor's Pick



View Online



Export Citation

## ARTICLES YOU MAY BE INTERESTED IN

### Chinese Abstracts

Chinese Journal of Chemical Physics **35**, i (2022); <https://doi.org/10.1063/1674-0068/35/03/cabs>

Comparative study of GaAs nanostructures synthesized in air and distilled water by picosecond pulsed laser ablation and application in hazardous molecules detection  
Journal of Laser Applications **34**, 032014 (2022); <https://doi.org/10.2351/7.0000750>

### Elastic interactions in physics are reflections in geometry

AIP Advances **12**, 085307 (2022); <https://doi.org/10.1063/5.0087903>



**JASA**  
THE JOURNAL OF THE  
ACOUSTICAL SOCIETY OF AMERICA

**Special Issue:**  
**Additive Manufacturing and Acoustics**

Read Now!

# Experimental measurements of a prototype vibraphone bar with three-dimensional cutaway geometry

Douglas Beaton  and Gary Scavone<sup>a)</sup>

Computational Acoustic Modeling Laboratory, Center for Interdisciplinary Research in Music Media and Technology,  
Schulich School of Music, McGill University, Montreal, Quebec H3A 1E3, Canada

[douglas.beaton@mail.mcgill.ca](mailto:douglas.beaton@mail.mcgill.ca), [gary.scavone@mcgill.ca](mailto:gary.scavone@mcgill.ca)

**Abstract:** This article discusses the fabrication and testing of two prototype vibraphone bars. Bar cutaway shapes vary along both the length and width of the bar, whereas previous examples in the literature vary only along the length. Bar shapes were designed using a method, previously published by the authors, that tunes both flexural and torsional modes. Fabrication issues prevented the first prototype from achieving its desired geometry. These issues were resolved in the second prototype, which accurately reflects its designed geometry and produces modal frequencies that agree well with design targets. © 2022 Author(s). All article content, except where otherwise noted, is licensed under a Creative Commons Attribution (CC BY) license (<http://creativecommons.org/licenses/by/4.0/>).

[Editor: Charles C. Church]

<https://doi.org/10.1121/10.0013470>

**Received:** 22 June 2022 **Accepted:** 26 July 2022 **Published Online:** 12 August 2022

## 1. Background and motivation

This article extends the work of [Beaton and Scavone \(2021\)](#) by providing experimental measurements to complement the previously reported theoretical results. Readers may refer to the original paper for terminology definitions, description of the tuning method, and discussion of its performance. The main distinguishing aspect of this method and the prototype bars described here are their three-dimensional cutaway geometries. Previous works in the idiophone literature have invariably produced bars with thickness that is uniform across the bar's width. In this work, bar geometry varies in all directions, creating a truly three-dimensional cutaway.

Previous examples of aluminum idiophone bars fabricated to match theoretical designs can be found in the literature. For brevity, the following examples consider only bars fabricated from aluminum. In all cases, bar geometries were designed using finite element analysis.

[Laukkanen and Worland \(2011\)](#) produced bars tuned *via* simple rectangular cuts. Their cuts were positioned at discrete points along the bar's length, rather than being limited to a more traditional contiguous cutaway. The cuts were simple enough to be fabricated using an endmill on a milling machine, rather than a computer numerically controlled (CNC) mill. Their two example designs tuned the first three vertical-flexural bar modes to ratios of 1:2:4 and 1:3:5, respectively. Modal frequencies of their fabricated bars, measured using electronic speckle pattern interferometry (ESPI), were stated to be within 1% ( $\approx 17$  cents) of their targets, though specific values were not reported.

[Kirkland and Moradi \(2016\)](#) used spline curves to define their bar cutaway profiles. The resulting cutaway profiles more closely resemble traditional vibraphone bars than do the rectangular cuts of [Laukkanen and Worland \(2011\)](#). The stated goal of [Kirkland and Moradi \(2016\)](#) was to find a cutaway geometry that minimizes bar mass while tuning the first three vertical-flexural modes to the traditional ratios of 1:4:10. Modal frequencies in their bar models were tuned to within a tolerance of 0.25% ( $\approx 4$  cents). Two identical bars were fabricated *via* CNC mill. Mallet strikes on the fabricated bars were recorded with a microphone. Modal frequencies were approximated by picking peaks from the recorded waveforms' spectra. [Kirkland and Moradi \(2016\)](#) report identical errors of  $-2$  cents for the fundamental frequencies of their two prototypes. Their stated accuracy of  $\pm 1.35$  Hz for the measured frequencies would place this error somewhere between  $-7.5$  cents and  $+3$  cents.

[Bestle et al. \(2017\)](#) also used spline curves to define bar cutaway profiles. Two different bars were designed and fabricated as part of a doctoral thesis ([Bestle, 2017](#)). The first bar used a "classic undercut," comprised of a middle section of uniform thickness and curved ends modelled as splines. Its first two vertical-flexural modes were tuned to frequency ratios of 1:4. The second bar's undercut was modelled by a spline over its entire length, with symmetry enforced by mirroring at the bar's midpoint. Its first three vertical-flexural modes were tuned to the typical 1:4:10 ratios. The two bars were fabricated *via* CNC mill. Experimental modal analysis (EMA) was used to measure modal frequencies of the fabricated bars. Modelled and measured frequencies are reported for the first seven modes of each bar, with a maximum error of 0.7% (12 cents). Fundamental frequencies are reported to be within 0.1% (2 cents).

<sup>a)</sup> Author to whom correspondence should be addressed.

TABLE 1. Aluminum material properties for bar fabrication compared with standard values. For fabrication: density,  $\rho$ , and Young’s modulus,  $E$ , were measured from stock material. The standard value of Poisson’s ratio,  $\nu$ , was adopted, while shear modulus,  $G$ , was calculated from  $E$  and  $\nu$  as:  $G = E \cdot [2(1 + \nu)]^{-1}$ . Standard aluminum properties are from the 6061 alloy (Battelle Memorial Institute, 2020).

Property	$\rho$ [kg/m <sup>3</sup> ]	$E$ [GPa]	$\nu$	$G$ [GPa]
For Fabrication	2693	69.39	0.33	26.09
Standard - 6061 Alloy	2700	68.90	0.33	25.90

Soares *et al.* (2021) defined cutaway geometries using stepped rectangular cuts similar to Laukkanen and Worland (2011) but generally contained in a contiguous region. Their models tuned both vertical-flexural and torsional mode types. Three bars were fabricated, each of which tuned six modes. The first four vertical-flexural modes were tuned to frequency ratios of 1:4:10:16 in all three cases. Two torsional modes were also tuned for each bar, with frequency ratios of either 4:16, 6:18, or 5:20. Bars were fabricated *via* CNC mill with a stated cutting accuracy of approximately  $\pm 0.05$  mm. Modal frequencies were measured *via* EMA. Soares *et al.* (2021) report errors of  $-26$ ,  $-12$ , and  $-38$  cents in the fundamental frequencies of the three fabricated bars.

## 2. Method

A description of the cutaway geometry parametrization and mathematical approach to bar tuning used here is provided by Beaton and Scavone (2021). The following sections describe procedures relevant to bar fabrication.

### 2.1 Materials

Bars were fabricated from the popular 6061 aluminum alloy (Battelle Memorial Institute, 2020). Stock material was purchased in 63.5 mm wide by 19 mm thick bars. Some material properties were measured to provide greater accuracy in bar performance. Density was measured by weighing and measuring the dimensions of the stock material. Young’s modulus was determined by performing EMA on a piece of stock material (see Sec. 2.4), and adjusting the Young’s modulus of a converged (see Sec. 2.2) model of the stock bar such that the fundamental frequency of the modeled bar matched the value measured *via* EMA. Poisson’s ratio was taken as 0.33, a commonly published value (Battelle Memorial Institute, 2020). Shear modulus was calculated from the measured Young’s modulus and adopted Poisson’s ratio. Table 1 outlines the material properties used for fabrication as compared to published values.

### 2.2 Model convergence

Once bar dimensions and target modal tuning ratios were selected, model convergence was assessed by varying the bar’s mesh density.

In finite element modeling, convergence checks generally involve tracking model outputs as progressively denser meshes are applied to given model geometry. Analysts use the resulting trends to determine the mesh density required to produce outputs within a given tolerance. A slightly different style of convergence check was employed in this work. Beginning with a coarse mesh of 20-node hexahedral elements, the tuning algorithm of Beaton and Scavone (2021) was run on models with progressively denser meshes. Each subsequent model began with the final geometry definition vector from the previous model. The model was considered converged when the final geometry definition vector from one model tuned all modes to within tolerance in the subsequent model. Thus, rather than assessing model results with progressively denser meshes of the same geometry, this convergence check assessed tuning algorithm output geometries, using models with progressively denser meshes.

A tolerance of  $\pm 1$  cent was used for all tuned modes in the finite element models. Figure 1 shows the models used in testing convergence for the second prototype bar, indicating the number of elements in each. The relative increase

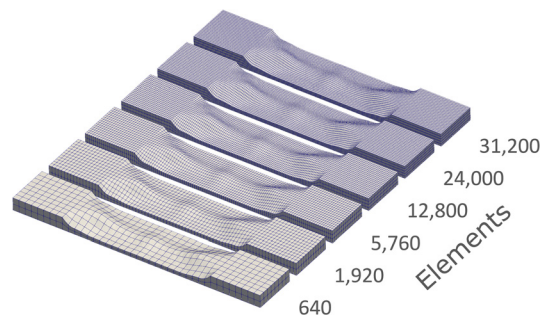


Fig. 1. Finite element meshes used to test convergence for the model of Prototype 2. Each structured mesh is comprised of 20-node hexahedral elements with uniform density throughout.

in element numbers diminishes as the models progress. Computer memory capacity limited the number of elements used in the final model.

### 2.3 Fabrication

Bar cutaways were carved using a Mazak Vertical Center Universal 400 5X five-axis CNC mill. Generally speaking, a five-axis CNC mill can position its cutting head relative to a machined part using three translational and two rotational axes. Different mills may move either the cutting head or the part itself, along a given axis. Depending on the complexity of a bar's cutaway geometry, it may be possible to use a simpler (e.g., three-axis) CNC mill. Such a choice should be informed by experienced CNC mill operators, with consideration given to factors such as available cutting tools and desired surface roughness.

A tolerance of  $\pm 0.025$  mm was specified for the fabricated bar geometry. Material was removed in multiple passes. Machining aluminum using cutting tools such as CNC mills will induce residual stresses, resulting in distortion of the bar [Wang et al. \(2018\)](#). For this reason, the bar's top side (playing surface) was planed after an initial rough milling of the cutaway shape. This was necessary to maintain a flat surface upon which to mount the bar in the CNC mill. Planing the bar thus removed additional material to compensate for the induced distortion. This step created problems for one prototype, as discussed in Sec. 3.1.

### 2.4 Measurements

Bar performance was assessed using EMA. Bars were supported using foam blocks placed roughly below the nodes of their first vertical-flexural mode. A Polytec PDV-100 laser Doppler vibrometer (Polytec, Waldbronn, Germany) (LDV) was positioned below the bar and aimed at the corner of the bar's bottom surface. A Brüel & Kjær type 8203 (Brüel & Kjær, Nærum, Denmark) impact hammer was used to excite a grid of strike points on the bar's top surface. Data were recorded and analyzed in MATLAB. Modal frequencies were computed using the *Least Squares Complex Exponential* (LSCE) method ([Brown et al., 1979](#)).

## 3. Bar performance

Two prototype bars were produced. The second bar was fabricated several weeks after, taking into account lessons learned during the first fabrication process. The following sections discuss the two prototypes separately, as their outcomes were decidedly different. The first fabricated bar, *Prototype 1*, was hindered by manufacturing problems. These issues are described below in hopes they may be instructive for future readers interested in machining aluminum on a CNC mill. Fortunately, the manufacturing problems that plagued Prototype 1 were overcome in producing the second bar, *Prototype 2*. Its design and manufacture are discussed in more detail as this bar is considered representative of bars that can be produced using the tuning method described by [Beaton and Scavone \(2021\)](#).

### 3.1 Prototype 1—Fabrication issues

Cutaways are carved on the bottom of a vibraphone bar, thereby maintaining a flat playing surface on top. Removing material from a single side of a bar in this manner can result in distortion (warping) of the bar due to unbalanced internal forces from residual stresses. Such imbalances can arise from two types of residual stresses: *inherent* and *machining-induced* ([Mathews et al., 2022](#)).

Inherent residual stresses (IRS) are present in the bar prior to machining, and may be a result of the stock bar's manufacture. Before machining, internal forces imparted by IRS are in equilibrium in the stock piece. Removing significant amounts of material to form the bar's cutaway disturbs the equilibrium of these internal forces, as material that previously carried a portion of these forces has been removed. The resulting force imbalance can thus induce distortion, as the bar deforms to re-establish internal force equilibrium.

Machining-induced residual stresses (MIRS) are imparted by the high temperatures and forces involved in the machining process ([Wang et al., 2018](#)). These newly imparted stresses can also cause an imbalance in internal forces, resulting in bar distortion.

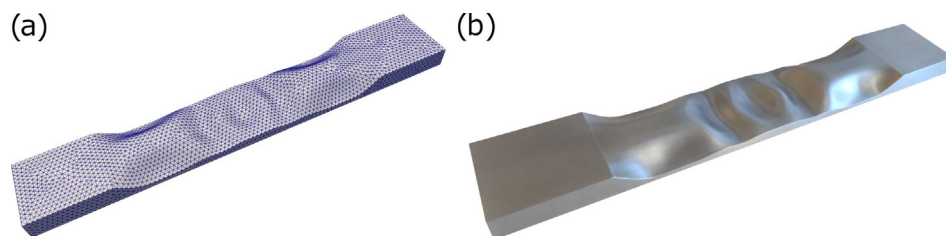


Fig. 2. Prototype 1 bar geometry: (a) meshed finite element model, (b) photo of fabricated bar.

Table 2. Prototype and stock bar outer dimensions.

Bar	Length [mm]	Width [mm]	End Thickness [mm]
Prototype 1	400	63.5	19
Prototype 2	365	63.5	18
Stock	459	63.5	19

Table 3. Modal tuning ratios for the two prototype bars. Label “V1” denotes the first vertical-flexural mode, while “T2” represents the second torsional mode, and so on. Untuned modes are indicated by “-.”

Bar	Tuning ratio					
	V1	V2	V3	T1	T2	T3
Prototype 1	1	4	10	4	14	—
Prototype 2	1	4	10	3	12	22

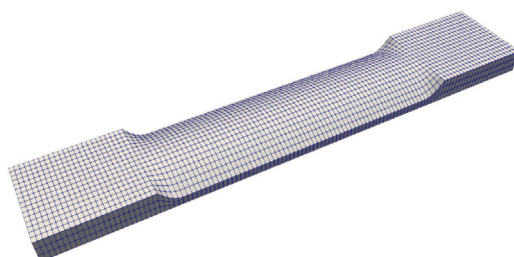


Fig. 3. Initial input bar geometry used to tune Prototype 2. The initial cutaway is thick along the centreline and thinned at the sides to reduce the likelihood of sharp edges appearing in the final tuned geometry. A similar initial geometry was used for Prototype 1.

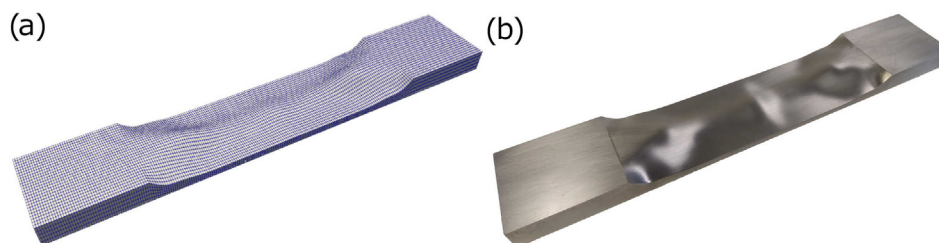


Fig. 4. Prototype 2 bar geometry: (a) meshed finite element model, (b) photo of the fabricated bar.

Table 4. Measured and modelled frequencies of the tuned modes in Prototype 2. Frequency errors are expressed in cents, relative to the modelled values. Measured frequency ratios are calculated relative to the measured frequency of mode V1.

Mode	Frequencies			Frequency ratios		
	Modelled [Hz]	Measured [Hz]	Error [cents]	Target	Measured	Error [cents]
V1	261.7	261.1	-4.1	1	1	—
T1	785.2	772.1	-29.1	3	2.96	-24.9
V2	1046.8	1047.2	0.7	4	4.01	4.6
V3	2616.3	2632.5	10.6	10	10.08	14.2
T2	3139.5	3108.7	-17.4	12	11.91	-13.6
T3	5755.8	5757.1	0.5	22	22.05	3.9

As discussed in Sec. 2.3, some material was removed from the prototype bars during fabrication to counteract distortion and maintain a flat working surface. Prototype 1, shown in Fig. 2, was designed with a width and thickness matching those of the stock bar (see Table 2). This left no excess material available for removal to compensate for bar distortion. As a result, Prototype 1's fabricated geometry was on the order of 0.5 mm too thin over a large portion of its length. Such a discrepancy was well outside the intended  $\pm 0.025$  mm tolerance for bar geometry. As one might expect, the resulting modal frequencies were nowhere near their intended values. These errors in modal frequency are not reported here, as they are clearly a product of manufacturing problems, not the tuning method (Beaton and Scavone, 2021) they were intended to validate.

### 3.2 Prototype 2—Accurate manufacture

Fabrication shop technicians collaborated in the second prototype bar's design to ensure accurate reproduction of the desired geometry. Most importantly, Prototype 2's end thickness was set at 1 mm less than the stock material's thickness. This provided flexibility in removing material to compensate for distortion induced by the fabrication process. The resulting bar much more accurately reflected its intended geometry than did Prototype 1. Table 2 gives the outer dimensions of both prototypes as compared to the stock materials from which they were fabricated.

Prototype 2's fundamental frequency was set to match musical note C4. A multitude of potential tuning ratio combinations was investigated. The bulk of these combinations maintained the typical 1:4:10 ratios in the first three vertical-flexural modes while tuning some further combination of torsional, vertical-flexural, and/or lateral-flexural modes. Bar length was also varied along with the tuning ratios to see which combinations would produce an interesting yet practical (for fabrication) cutaway shape. Table 3 outlines the modal tuning ratios used to design the prototype bars.

When using three-dimensional cutaway geometries to tune idiophone bars, it is possible for undesirable sharp edges or rapidly fluctuating geometries to appear (see, for example, model 3 from Beaton and Scavone (2021)). A benefit of the tuning approach employed here is that final cutaway geometries tend toward similarity to initial input geometries. Thus, to avoid sharp edges in the prototype designs, the tuning algorithm was supplied with an initial cutaway geometry that was thick along the bar's centreline and thinned at its edges. Figure 3 shows the initial bar geometry used to tune Prototype 2's cutaway shape. The final design geometry is shown in Fig. 4, along with a photo of the fabricated bar. As is evident in Fig. 4, the final geometry has no sharp ridges and relatively gradual changes in slope throughout the cutaway.

Table 4 shows the resulting performance of Prototype 2 in terms of tuned modal frequencies. To facilitate comparison with other results in the literature, errors are reported for both frequencies and frequency ratios. Measured frequency ratios are calculated relative to the measured frequency of mode V1.

Overall the measured modal frequencies in Table 4 show good agreement with modelled values. An error of  $-4.1$  cents in the fundamental frequency is comparable to examples from the literature in Sec. 1. Generally speaking, the vertical-flexural modes show better agreement with modelled values than do the torsional modes. Measurement conditions may play a factor here, as the foam blocks upon which the bar rested may have had some effect on the torsional modes. Notably, within each type of mode (vertical-flexural, or torsional), frequency errors become more positive with increasing mode number. From mode V1 to V2, frequency error becomes more positive; the same is true from mode V2 to V3, T1 to T2, and T2 to T3. Mode V2 shows the lowest magnitude frequency error of the three tuned vertical-flexural modes. Mode T3 shows the lowest magnitude frequency error of all six tuned modes.

## 4. Concluding remarks

The two fabricated prototype bars described in Sec. 3 presented vastly different outcomes. Prototype 1 was plagued by production issues, resulting in a fabricated bar geometry that departed significantly from its design. While not visually apparent in Fig. 2, a roughly 0.5 mm reduction in bar thickness has a large impact on modal frequencies. Though clearly not a successful example, fabrication of Prototype 1 is included here in the hopes it may be instructive to readers in their own work.

Fortunately, Prototype 2 fared much better than Prototype 1. Prototype 2 much more accurately realizes its intended design geometry. As a result, the errors in measured vs modelled modal frequencies shown in Table 4 are comparable to other examples of fabricated vibraphone bars in the literature. Prototype 2 thus serves to validate the tuning method of Beaton and Scavone (2021), and demonstrates the potential of three-dimensional cutaway shapes to concurrently tune vertical-flexural and torsional bar modes.

## Acknowledgments

This research was supported by the Vanier Canada Graduate Scholarships program. The authors would also like to thank Ramnarine Harihar, Meisam Aghajani and Andreas Hofmann at McGill's Mechanical Engineering Workshop for their assistance in fabricating the prototype bars.

## References and links

Battelle Memorial Institute (2020). *Metallic Materials Properties Development and Standardization (MMPDS-15)* (Battelle Memorial Institute, Columbus, OH).

- Beaton, D., and Scavone, G. (2021). "Three-dimensional tuning of idiophone bar modes via finite element analysis," *J. Acoust. Soc. Am.* **149**(6), 3758–3768.
- Bestle, P. (2017). *Zur Klangoptimierung Von Idiophonen Mittels Schallsynthetisierung (For Sound Optimization of Idiophones by Means of Sound Synthesis), Number 52 in Schriften Aus Dem Institut Für Technische und numerische mechanik Der Universität Stuttgart* (Shaker Verlag, Aachen, Germany).
- Bestle, P., Eberhard, P., and Hanss, M. (2017). "Musical instruments—Sound synthesis of virtual idiophones," *J. Sound Vib.* **395**, 187–200.
- Brown, D. L., Allemang, R. J., Zimmerman, R., and Mergeay, M. (1979). "Parameter estimation techniques for modal analysis," *SAE Trans.* **88**(1), 828–846.
- Kirkland, W. B., and Moradi, L. (2016). "Topographical optimization of structures for use in vibraphones and other applications," in *Proceedings of the Society for Design and Process Science 21st International Conference*, December 4–6, Orlando, FL, pp. 69–77.
- Laukkanen, E. M., and Worland, R. (2011). "Acoustical effect of progressive undercutting of percussive aluminum bars," *Proc. Mtgs. Acoust.* **14**(1), 025003.
- Mathews, R., Sunny, S., Malik, A., and Halley, J. (2022). "Coupling between inherent and machining-induced residual stresses in aluminum components," *Int. J. Mech. Sci.* **213**, 106865.
- Soares, F., Antunes, J., and Debut, V. (2021). "Tuning of bending and torsional modes of bars used in mallet percussion instruments," *J. Acoust. Soc. Am.* **150**(4), 2757–2769.
- Wang, J., Zhang, D., Wu, B., and Luo, M. (2018). "Prediction of distortion induced by machining residual stresses in thin-walled components," *Int. J. Adv. Manuf. Technol.* **95**(9–12), 4153–4162.